Analytica Chimica Acta 693 (2011) 114–120

Contents lists available at ScienceDirect

Analytica Chimica Acta

journal homepage: www.elsevier.com/locate/aca

A novel biosensing mechanism based on a poly(*N*-butyl benzimidazole)-modified gold electrode for the detection of hydrogen peroxide

Mu-Yi Hua [a,b,*], Hsiao-Chien Chen [a,b], Rung-Ywan Tsai [c], Yu-Chen Lin [a,b], Leeyih Wang [d]

[a] Green Technology Research Center, Department of Chemical and Materials Engineering, Chang Gung University, Tao-Yuan 33302, Taiwan, ROC
[b] Biosensor Group, Biomedical Engineering Research Center, Chang Gung University, Tao-Yuan 33302, Taiwan, ROC
[c] Electronics and Optoelectronics Research Laboratories, Industrial Technology Research Institute, Hsinchu 31040, Taiwan, ROC
[d] Center for Condensed Matter Science, Institute of Polymer Science and Technology, National Taiwan University, Taipei 10617, Taiwan, ROC

ARTICLE INFO

Article history:
Received 18 December 2010
Received in revised form 7 March 2011
Accepted 8 March 2011
Available online 16 March 2011

Keywords:
Biosensor
Hydrogen peroxide
Peracetic acid
Poly(*N*-butyl benzimidazole)
Poly(*N*-butyl benzimidazole) *N*-oxide

ABSTRACT

A novel mechanism to detect hydrogen peroxide (H_2O_2) using a poly(*N*-butyl benzimidazole) (PBBI)-modified gold (PBBI/Au) electrode is proposed. Synthetic PBBI was oxidized using a mixture of acetic acid (AcOH) and H_2O_2 to form PBBI *N*-oxide (PBBINO). The structure of PBBINO was verified by Fourier transform infrared spectroscopy (FT-IR) and the degree of oxidation was measured by X-ray photoelectron spectroscopy (XPS). Moreover, the oxide could be reduced electrochemically back to PBBI. Based on this reaction, a novel enzyme-free PBBI/Au electrode was developed to detect H_2O_2 in the presence of AcOH electrochemically. The biosensor detected H_2O_2 linearly over concentrations ranging from 25 μM to 10 mM with a detection limit of 6.25 μM in phosphate buffer solution (PBS) mixed with AcOH at pH 6.4. In addition, at an applied potential of −0.5 V, the sensor characteristics could be tuned using AcOH over a pH range of 3.7–6.4. The sensitivity of the probe could be enhanced from 35.1 to 419.4 μA mM^{-1} cm^{-2} by modifying the surface morphology of the PBBI/Au electrode from a smooth plane to a granular, three-dimensional configuration. Furthermore, it was not influenced by interfering compounds and showed high thermal stability.

1. Introduction

H_2O_2, a chemical used widely in the food, pharmaceutical, paper, and chemical industries, is a reactive oxygen species that can cause cancer when found in excess in the human body [1]. It is also a by-product of the reaction catalyzed by large number of oxidase enzymes [2,3]. The detection of H_2O_2 thus is important in biomedical and environmental applications. In past decades, a number of technologies such as titrimetry, fluorescence, and absorbance spectra [4,5] have been developed to detect H_2O_2. Recently, a new generation of sensors based on electrochemical technology has proven simple to use and highly sensitive for real-time detection [6,7]. Most of the electrochemical methods are based on enzymes such as horseradish peroxidase, hemoglobin, or myoglobin [8–10]. Enzymatic electrodes usually are prepared by immobilizing a coat of enzymes mixed with organic or inorganic materials on the electrode surface. Although such biosensors are highly sensitive, loss of content and degradation lead to decreased enzyme activity over time. The development of enzyme-free biosensors to overcome this limitation is of great interest. The simplest alternative method is to electrocatalyze H_2O_2 directly at working potentials of 0.5–0.7 V [11–13]. Unfortunately, at this relatively high potential, the selectivity is easily influenced by the presence of interfering species [14].

Recently, electrodes modified with inorganic and organic–inorganic materials have been studied widely owing to their selectivity, stability, and the efficiency with which they transfer electrons; such modifications include metallic particles (Ag, Au, Co, and CuS nanoparticles) [15–17], metallic oxides (Cu_2O, CuO, TiO_2, and MnO_2) [18–21], transition metals (Prussian blue and metalloporphyrins) [22,23], and biological complexes incorporating inorganic components [24]. Such polymer-modified electrodes, either with immobilized enzymes or with hybrid organic–inorganic compounds, are widely used because of their high build and ease of preparation [25,26]. However, only a few studies have used polymers without enzymes to detect H_2O_2 at lower potentials [27,28].

Polybenzimidazole (PBI) is a heterocyclic aromatic polymer with exceptional chemical resistance, excellent mechanical strength, and thermal stability [29,30]. After doping with acid, it is an excellent proton conductor and is used in proton exchange membranes in fuel cells [31,32]. Furthermore, its fluorescence char-

* Corresponding author at: Green Technology Research Center, Department of Chemical and Materials Engineering, Chang Gung University, Tao-Yuan 33302, Taiwan, ROC. Tel.: +886 3 2118800x5289; fax: +886 3 2118668.
E-mail address: huamy@mail.cgu.edu.tw (M.-Y. Hua).

0003-2670/$ – see front matter © 2011 Elsevier B.V. All rights reserved.
doi:10.1016/j.aca.2011.03.020

acteristics – the result of benzimidazole's conjugated structure – have been investigated and reported widely [33]. PBI is poorly soluble in many solvents because of its rigid backbone and interchain interactions via hydrogen bonds. Alkylation of PBI improves its solubility without sacrificing its original properties [34]. However, neither PBI nor its derivatives have been used to modify electrodes for biosensor applications.

Here, we demonstrate that PBBI prepared by the butyl alkylation of PBI with 1-iodobutane can be oxidized by peracetic acid (a mixture of AcOH and H_2O_2; AcOOH) to form PBBINO, which subsequently can be reduced electrochemically. Based on this reaction, a PBBI/Au electrode was developed for use as an enzyme-free H_2O_2 biosensor. This biosensor showed superior performance compared with traditional ones, including long-term detection capability, rapid response time, and high specificity. Furthermore, preparing a three-dimensional PBBI/Au (3D-PBBI/Au) electrode with a granulated surface enhanced the sensitivity of the probe to 12 times that of a PBBI/Au electrode with a smooth surface. We also propose the redox mechanism by which the PBBI/Au electrode detects H_2O_2.

2. Experimental

2.1. Chemicals

Isophthaloyl dichloride (98%) was purchased from Acros, 3,3′-diaminobenzidine tetrahydrochloride hydrate (>97%) was from Sigma–Aldrich, polyphosphoric acid and H_2O_2 (30%) were from Showa, dimethyl sulfoxide (DMSO) was from Tedia, sodium hydride was from Fluka, 1-iodobutane (99%) was from Lancaster, and AcOH (99.8%) was from Scharlau. Deionized (DI) water was used in all experiments.

2.2. Instrumentation and measurements

FT-IR spectra were obtained using a Bruker-Tensor 27 spectrometer at a spectral resolution of 8 cm^{-1}. XPS measurements were performed using a VG Scientific ESCALAB 250 system. Electrochemical measurements were performed on a CHI 660A electrochemical workstation (CH Instruments, USA) with a three-electrode system consisting of the PBBI/Au electrode, a bare Au electrode, and an Ag/AgCl electrode as the working, counter, and reference electrodes, respectively. All electrochemical measurements were performed in 40 mL of 0.2 M PBS at 25 °C and at pH 7.0 (unless stated otherwise). The pH values of the electrolytes were adjusted with AcOH to 7.0 (without AcOH), 6.4 (43.8 mM AcOH), 4.6 (216.0 mM AcOH) or 3.7 (833.4 mM AcOH).

2.3. Procedures

2.3.1. Preparation of PBI, PBBI, and PBBINO

PBI was synthesized by condensation of 3,3′-diaminobenzidine tetrahydrochloride hydrate and isophthaloyl dichloride in polyphosphoric acid [35]. To produce PBBI, 1 mmol of PBI (0.3 g) was dissolved in 50 mL of DMSO and stirred at 80 °C for 1 h. Sodium hydride (0.1 g; 4.2 mmol) was added and the solution was purged with nitrogen to form a deep red solution. After stirring for 2 h, 0.55 g (3 mmol) of 1-iodobutane was added and reacted for 24 h at 120 °C. The solution was added to 500 mL of DI water, stirred vigorously, and the precipitate was separated from the solution by filtration. The filtered solid was redissolved in DMSO, recrystallized sequentially three times with acetone, and dried in a vacuum aspirator to obtain the PBBI.

AcOOH solutions were prepared by mixing 0.2 mmol AcOH with 0.1, 0.2, or 0.4 mmol H_2O_2. PBBI (0.2 mmol) was dissolved in 10 mL of DMSO and added to the AcOOH solutions. The reactions were incubated in a 43-kHz ultrasonic bath at 40 °C for 0.5 h in a dark room. The purification procedure was as described above for PBBI, producing PBBINO1, PBBINO2, and PBBINO3, with molar ratios of PBBI:AcOH:H_2O_2 of 1:1:0.5, 1:1:1 and 1:1:2, respectively.

2.3.2. Preparation of the PBBI/Au and 3D-PBBI/Au electrodes

To produce the PBBI/Au electrode, 2 μL of a solution containing 0.23 g PBBI in 10 mL of DMSO were dropped onto an Au disk electrode (0.196 cm^2) and dried in a vacuum aspirator at 50 °C for 5 h. The 3D-PBBI/Au electrode was similarly prepared by dissolving 0.23 g PBBI in 10 mL of DMSO and then dispersing it with stirring into a poor solvent consisting of 250 mL DI water and 150 mL acetone. After high-speed centrifugation (5500 rpm), the precipitate was washed by DI water three times. Finally, the precipitate was dispersed into 40 mL DI water and 4 μL of the solution with 1% DMSO was dropped onto an Au disk electrode (0.196 cm^2) and dried in a vacuum aspirator at 50 °C for 5 h.

3. Results and discussion

3.1. Characterization of PBBI and PBBINO

FT-IR spectroscopy detected the characteristic absorption bands of PBBI (Fig. 1A), including the stretching vibrations (ν) of N–H (ν_{N-H}) at 3389 cm^{-1}, unsaturated ν_{C-H} (3061 cm^{-1}), asymmetric and symmetric saturated ν_{C-H} (2931 and 2864 cm^{-1}, respectively), $\nu_{C=N/C=C}$ (1617 cm^{-1}), the in-plane deformation of benzimidazole (1558 cm^{-1}), and C–H bending (1457 and 1389 cm^{-1}). Two other peaks appearing at 801 and 701 cm^{-1} were indicative of heterocyclic ring vibrations [36]. After reacting with AcOOH, three new peaks attributable to the resonance structure of PBBINO1 appeared at 1709 cm^{-1} ($\nu_{C=N^+}$), 1204 cm^{-1} ($\nu_{N^+-O^-}$), and 1050 cm^{-1} (benzene ring in-plane C–H bending) (Fig. 1A) [37]. Furthermore, the intensity of the latter two peaks increased with increasing concentrations of H_2O_2 at a constant concentration of AcOH (Fig. 1A). However, oxidation did not occur in the absence of AcOH. This is consistent with the results seen when pyridine is added to a mixture of AcOH and H_2O_2 to produce pyridine *N*-oxide [38], indicating that PBBINO is formed through the oxidation of PBBI by AcOOH (a mixture of H_2O_2 and AcOH).

The N(1s) XPS spectrum of PBBI can be deconvoluted into three peaks (Fig. 1B): imine at 398.4 eV, amine at 400.2 eV, and a peak at 400.3 eV attributable to the amine substitution by butyl alkylation [39]. The ratio of the peak areas was 1:0.55:0.45; *i.e.*, butyl alkylation accounted for 45%, whereas 55% remained as native amine. The N(1s) spectrum of PBBINO3 (Fig. 1B) was deconvoluted into four peaks: in addition to the previous three peaks, a new characteristic peak formed at 402.0 eV, indicating formation of the *N*-oxide structure (imine salt) [40]. The ratio of the peak areas (from lowest to highest binding energy) was 8.60:27.24:22.60:41.56. Thus, the corresponding ratios of amine N (native amine plus butyl amine):imine N:imine salt was 1.00:0.17:0.83; *i.e.*, the total area of imine N and imine salt was equal to that of amine N. Consistent with the results of the FT-IR studies, the XPS spectra suggest that the reactive site occurring at the imine of PBBI can be oxidized by AcOOH to form an imine salt, which in PBBINO3 accounts for 41.5% of the total area attributable to N.

3.2. Electrochemistry of the PBBI/Au electrode

Cyclic voltammograms of the PBBI/Au electrode showed one pair of redox peaks between −0.6 and 0.6 V at a potential scan rate (υ) of 0.05 V s^{-1} in PBS at pH 7.0 (Fig. 2A). The potentials of the anodic (E_{pa}) and cathodic (E_{pc}) peaks were 0.20 and 0.04 V, respectively, with a peak-to-peak separation ((E_p) of 0.16 V and a formal potential (the average of E_{pa} and E_{pc}; $E^{0'}$) of 0.12 V. This

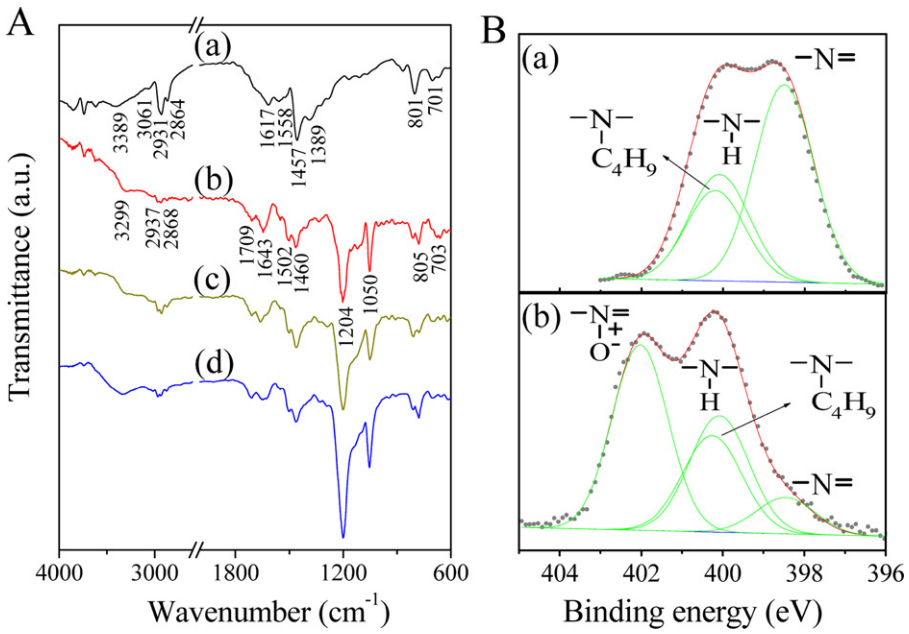

Fig. 1. (A) FT-IR spectra of (a) PBBI, (b) PBBINO1, (c) PBBINO2, and (d) PBBINO3. (B) N(1s) XPS spectra of (a) PBBI and (b) PBBINO3. –N=: imine; $\overset{-N-}{\underset{H}{|}}$: amine; $\overset{-N-}{\underset{C_4H_9}{|}}$: amine-substituted PBBI; $\overset{-N=}{\underset{O^-}{|^+}}$: imine salt.

pair of peaks is characteristic of electroactive imine. In 0.2 M PBS at pH 7.0, both the anodic and the cathodic peak currents of the of PBBI/Au electrode increased with increasing υ (Fig. 2B) and were linearly proportional to the square root of υ over a range from 0.05 to 0.3 V s^{-1} (Fig. 2C), indicating that the electrochemical response of the PBBI/Au electrode is a typical diffusion-controlled process. Meanwhile, the low conductivity of PBBI (which cannot respond instantly at high υ because of the slow electron transfer rate) and the distortion in the aromatic backbone caused by alkylation resulted in positive and negative shifts of E_{pa} and E_{pc}, respectively, as υ increases [41]. Furthermore, when (E_p is >0.2 V and υ > 0.1 V s^{-1}, the peak potentials were proportional to the natural logarithm of υ (Fig. 2D). Two linear equations for the anodic (E_{pa} = 0.45 + 0.058 ln υ) and cathodic peak potentials

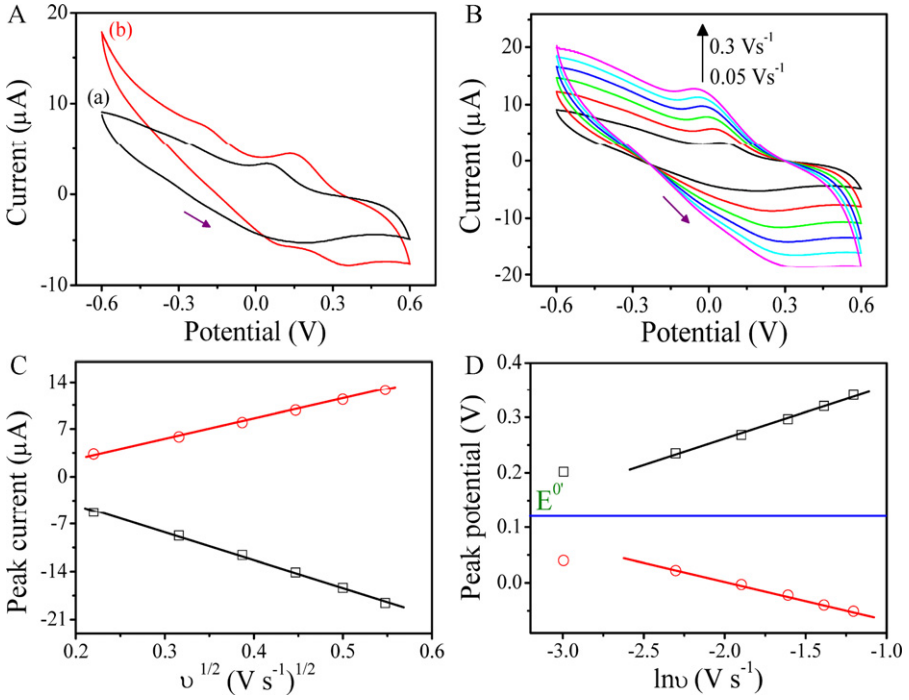

Fig. 2. (A) Cyclic voltammograms of the PBBI/Au electrode in 0.2 M PBS at (a) pH 7.0 and (b) pH 4.6. (B) Cyclic voltammograms of the PBBI/Au electrode in 0.2 M PBS (pH 7.0) as a function of υ (0.05–0.3 V s^{-1}). (C) Plots of peak currents *versus* the square root of υ. (D) Plots of peak potentials *versus* the natural logarithm of υ.

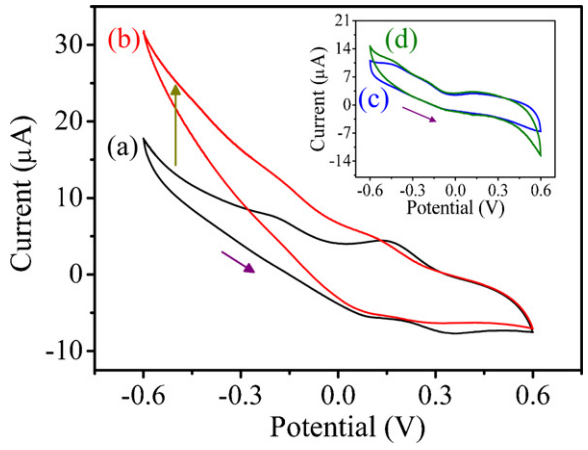

Fig. 3. Cyclic voltammograms of the PBBI/Au electrode in the (a) absence and (b) presence of 3 mM H_2O_2 in PBS at pH 4.6. Inset: cyclic voltammograms of a bare Au electrode in the (c) absence and (d) presence of 3 mM H_2O_2 in PBS at pH 4.6.

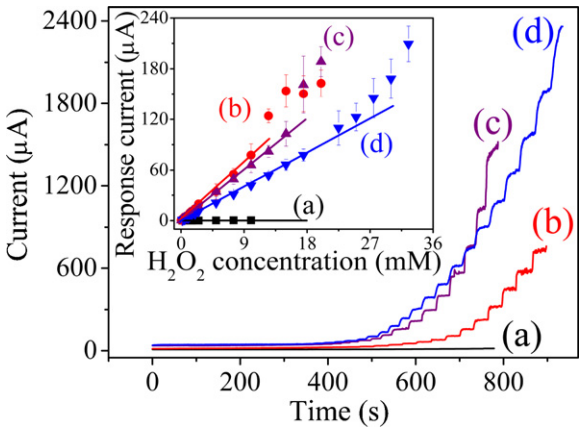

Fig. 4. Typical current/time response curves of the PBBI/Au electrode with the addition of different concentrations of H_2O_2 in PBS at (a) pH 7.0, (b) pH 6.4, (c) pH 4.6, and (d) pH 3.7. Inset: linear dependence of the response current *versus* the H_2O_2 concentration as a function of the pH of PBS: (a) pH 7.0, (b) pH 6.4, (c) pH 4.6, (d) pH 3.7 ($n = 5$).

($E_{pc} = -0.13 - 0.041 \ln \upsilon$) were obtained, respectively. According to Eq. (1) [42]:

$$\alpha = \frac{k_a}{k_a - k_c} \quad (1)$$

where α is the electron transfer coefficient and k_a and k_c are the slopes of E_{pa} and E_{pc} *versus* $\ln \upsilon$, respectively, the α of the PBBI/Au electrode in 0.2 M PBS (pH 7.0) was calculated to be 0.59. In principle, the number of transferred electrons (n) is equal to 1 when $0.3 < \alpha < 0.7$ [43]. Thus, the electrochemical reaction of PBBI in 0.2 M PBS appears to be a one-electron transfer process. Additionally, the surface concentration (Γ) of electroactive imine can be deduced according to Eq. (2) [44]:

$$I_p = \frac{n^2F^2d\upsilon A\Gamma}{4RT} \quad (2)$$

where I_p is the peak current, A is the surface area of the electrode (0.196 cm^2), F is Faraday's constant, and T is the temperature. In this case, the Γ of electroactive imine on the PBBI/Au electrode was estimated to be 7.4×10^{-10} mol cm^{-2}.

Because the oxidation of PBBI with H_2O_2 occurred in the presence of AcOH, the PBBI/Au electrode was also studied in acidic PBS. When the pH of the PBS was adjusted with AcOH to 4.6 (Fig. 2A), the peaks of electroactive imine shifted positively toward potentials of 0.35 V (E_{pa2}) and 0.13 V (E_{pc2}), respectively, with a (E_p of 0.22 V, presumably as a result of solution polarity. Furthermore, an additional pair of weak redox peaks appeared concurrently at 0.072 V (E_{pa1}) and −0.177 V (E_{pc1}). These likely resulted from redox reactions in which the imine of PBBI was partially protonated by the acidic solution [31,32].

To investigate the performance of the PBBI/Au electrode with respect to H_2O_2, cyclic voltammograms of the electrode were measured in PBS at pH 4.6 without and with the addition of 3 mM H_2O_2 (Fig. 3). Adding H_2O_2 increased the reductive current from 0 to −0.6 V, and the increase in the response current at −0.5 V was 12.3 μA. In contrast, adding the same concentration of H_2O_2 to the PBS at pH 4.6 did not induce an obvious current response in the bare Au electrode (Fig. 3, inset). Presumably, the imine sites of PBBI are oxidized by the hydroxyl radicals from AcOOH, forming the imine salt. When the imine salt content increases, more current is needed to reverse the process by electrochemical reduction. This is similar to the behavior seen in enzymatic and other enzyme-free biosensors in which the oxidation of substances by H_2O_2 is reversed by electrochemical reduction [8,20].

3.3. PBBI/Au electrode-based H_2O_2 biosensor

The above results indicate that PBBI could be oxidized by H_2O_2 to form PBBINO and generate a response current at reduction potentials from 0 to −0.6 V in the presence of AcOH. To assess the performance of PBBI/Au electrode as a means of assaying for H_2O_2, current/time plots were generated by the successive addition of H_2O_2 in PBS at varying pH values. To assure that the reduction reaction went to completion, an applied potential of −0.5 V (*i.e.*, more negative than that of the reductive peak) was used. At pH 7.0 (Fig. 4), the response current curve was negligible, indicating that PBBI was barely oxidized by H_2O_2 in the absence of AcOH. Although enzyme-free H_2O_2 biosensors are sensitive to oxygen production during H_2O_2 reduction at negative potentials [17], in this study no such current response occurred in the presence of H_2O_2 at pH 7.0, indicating that H_2O_2 was not reduced to oxygen. In contrast, the response currents increased markedly with increasing H_2O_2 concentrations at pH values of 6.4, 4.6 and 3.7 and achieved 95% of the steady-state current within 11.3, 6.0 and 4.9 s, respectively (Fig. 4). The corresponding calibration plots for the amperometric response curves and the biosensor performances at various pH values are presented in Fig. 4 (inset) and Table 1, respectively. Although the response time of the PBBI/Au biosensor was longest at pH 6.4, these conditions also produced the highest sensitivity and the lowest detection limit for H_2O_2. Indeed, over five trials using the same PBBI/Au electrode in PBS at pH 6.4, the sensor detected H_2O_2 over a linear range from 25 μM to 10 mM with a sensitivity of 35.1 μA mM^{-1} cm^{-2} and a standard deviation for the detection of 1 mM H_2O_2 of 3.9%.

The response time of the PBBI/Au biosensor is relative to the formation rate of AcOOH. At pH 6.4, the low concentration of AcOH reduces the opportunity for interactions with H_2O_2, resulting in a longer time required to achieve equilibrium. In contrast, sensitivity is dominated by the surface concentration of imine, which provides active sites to react with AcOOH. However, imine sites are also proton acceptors and are easily protonated in the acid solution [31,32]. As the AcOH concentration increases, so does the degree of protonation, reducing the surface concentration of imine that can react with AcOOH. Therefore, the sensitivity of the PBBI/Au electrode-based H_2O_2 biosensor decreases with increasing AcOH concentrations (and decreasing pH values). Consequently, a three-step mechanism is proposed as the basis for an enzyme-free PBBI/Au electrode to detect H_2O_2 (Scheme 1). Firstly, the mixture of AcOH and H_2O_2 in PBS produces AcOOH and H_2O. The AcOOH then oxidizes PBBI to

Table 1
Characteristics of the PBBI/Au electrode-based H_2O_2 biosensor in 0.2 M PBS at various pH values.

pH	Sensor characteristic				
	Response time (s)	Sensitivity ($\mu A\,mM^{-1}\,cm^{-2}$)	Detection range (mM)	Detection limit (μM)	*R*
3.7	<4.9	21.7	0.2–22.5	75.00	0.997
4.6	<6.0	33.2	0.075–15.0	12.50	0.998
6.4	<11.3	35.1	0.025–10.0	6.25	0.999
7.0	–	–	–	–	–

–: no response detected.

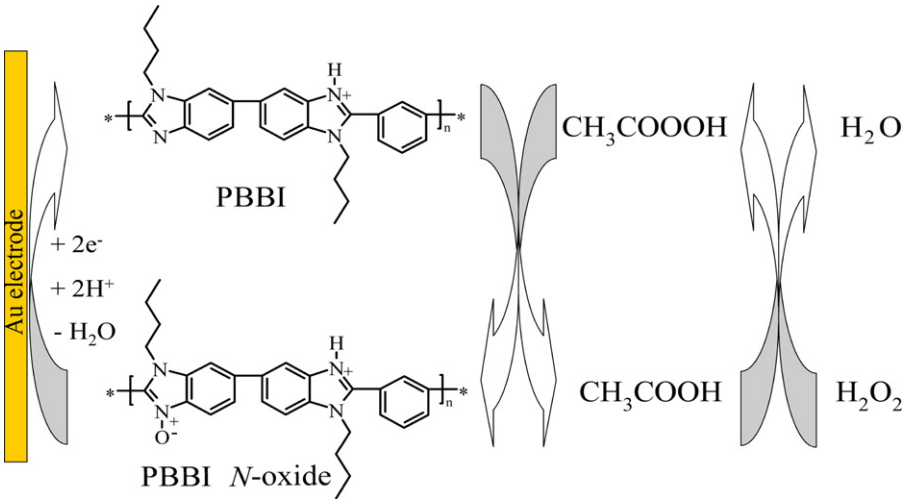

Scheme 1. Redox mechanism of the H_2O_2 biosensor using the PBBI/Au electrode as the working electrode.

form PBBINO and AcOH. Finally, the PBBINO reverts to PBBI and H_2O by accepting two electrons and two protons by electrochemical reduction. No PBBI is consumed at any point in the redox reaction, confirming the catalysis nature of the PBBI/Au electrode.

3.4. 3D-PBBI/Au electrode-based H_2O_2 biosensor

The above results demonstrate that a method to detect H_2O_2 using a PBBI/Au electrode is feasible and accurate. However, the solubility of the PBBI polymer in DMSO resulted in a planar morphology on the PBBI/Au electrode surface (Fig. 5A), limiting the effective surface area for detection. Therefore, a PBBI/Au electrode with a granulated surface and porous structure (Fig. 5A) was prepared by dispersing the PBBI in water before it was drop-coated onto the Au electrode. Current/time plots of the 3D-PBBI/Au electrode showed a rapid response, reaching 95% of the steady-state current in ~6.3 s (Fig. 5B), presumably because AcOOH could diffuse through the granulated surface freely. As with the PBBI/Au elec-

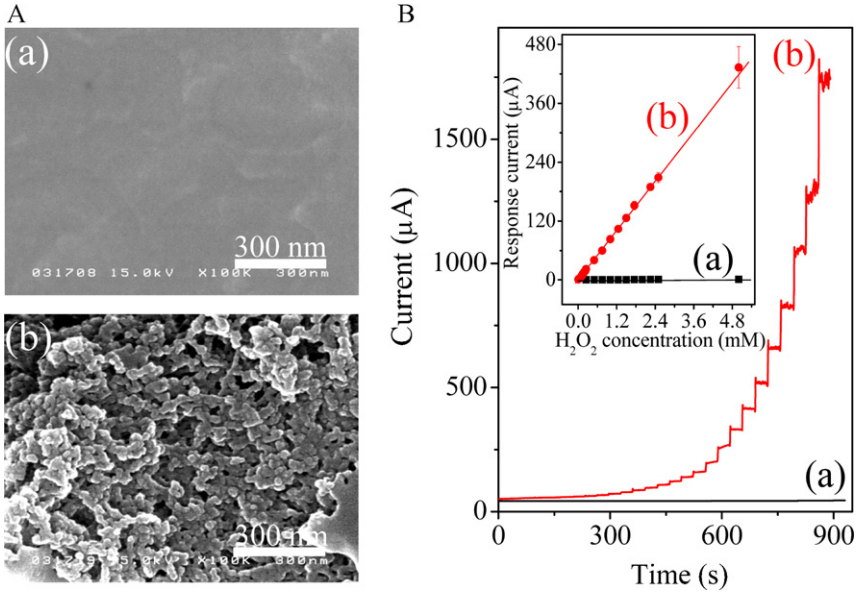

Fig. 5. (A) Scanning electron micrographs of (a) PBBI/Au electrode and (b) 3D-PBBI/Au electrode. (B) Typical current/time response curves of the 3D-PBBI/Au electrode at (a) pH 7.0 and (b) pH 6.4. Inset: linear dependence of the response current *versus* the H_2O_2 concentration ($n = 5$).

Table 2
Comparison of the performance of various H_2O_2 biosensors.

Modified electrode	Detection range	Sensitivity ($\mu A\,mM^{-1}\,cm^{-2}$)	Response time (s)	Ref.
Gel/HRP/TTF–TCN/MWCNTs/Au	5 μM–1.05 mM	383.0	6.0	46
MWCNTs/Ag/Au	50 μM–17 mM	20.1	5.0	47
Hb/SA/MWCNTs/GC	40 μM–0.2 mM	224.6	10.0	48
MnO_2/Nf/GC	10 μM–0.15 mM	–	5.0	49
Cu_2O/Nf/GC	5 μM–1.5 mM	717.1	3.0	19
3D-PBBI/Au	12.5 μM–5.0 mM	419.4	6.3	This work

HRP: horseradish peroxidase; TTF–TCN: tetrathiafulvalene–tetracyanoquinodimethane; MWCNTs: multiwalled carbon nanotubes; Hb: hemoglobin; SA: sodium alginate; GC: glassy carbon; Nf: Nafion.

trode, no response current was observed in the absence of AcOH (Fig. 5B). The linear range of the 3D-PBBI/Au electrode-based H_2O_2 sensor was 12.5 μM–5.0 mM with a slope of 419.4 $\mu A\,mM^{-1}\,cm^{-2}$ (Fig. 5B, inset) and a detection limit of 6.25 μM. Relative to the PBBI/Au electrode, the 3D electrode showed higher sensitivity (~12 times greater), a more rapid response and a lower detection limit.

3.5. Selectivity and stability of the 3D-PBBI/Au electrode H_2O_2 biosensor

Ascorbic acid (AA) and uric acid (UA) are often used to test for interference in H_2O_2 or glucose biosensors because they occur naturally in the body [14,15]. AA and UA are oxidized directly at potentials of 0.25 and 0.54 V, respectively [45]. Thus, the ability to detect H_2O_2 at negative potentials would avoid the effects of such interfering compounds. Indeed, at an applied potential of −0.5 V, neither AA nor UA at concentrations of 0.1–1 mM interfered noticeably with the response of the 3D-PBBI/Au electrode to H_2O_2 (Fig. 6A). Similarly, injecting 40 μL of PBS saturated with oxygen produced no obvious variation in the response current, indicating that the 3D-PBBI/Au electrode is specific for H_2O_2.

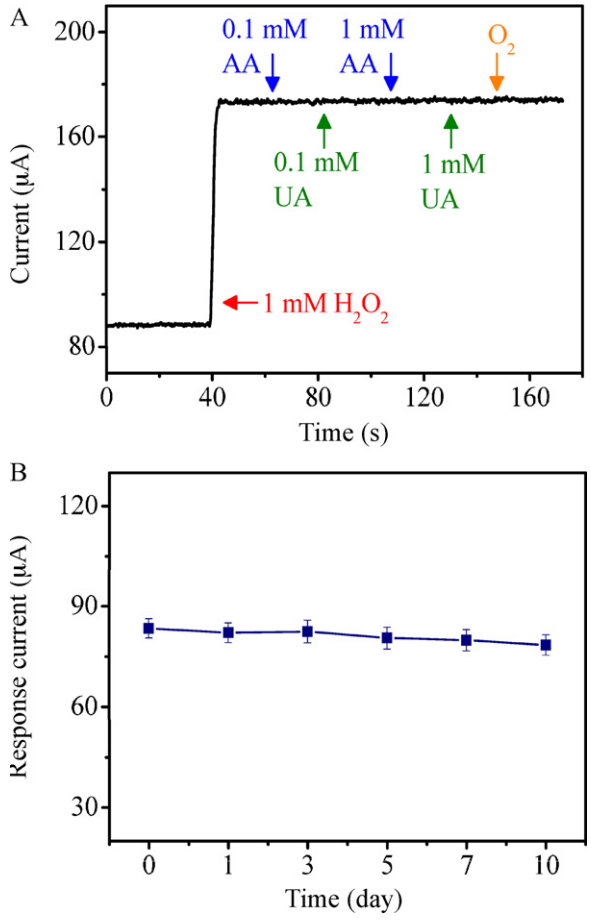

Fig. 6. (A) Influence of interfering substances on the response currents of the 3D-PBBI/Au electrode after the addition of 1 mM H_2O_2 in PBS at pH 6.4. (B) Variation of 3D-PBBI/Au electrode response currents in the presence of 1 mM H_2O_2 in PBS at pH 6.4 *versus* storage time at 50 °C.

The long-term stability of the 3D-PBBI/Au electrode was investigated by storing it at 50 °C in the atmosphere. The electrode showed very good stability, with a deviation after 10 days under such conditions of ≤5.9% from its initial response current (Fig. 6B). This excellent stability was attributed to the intrinsic thermal stability of PBBI.

The performance of the 3D-PBBI/Au electrode was comparable to that of other H_2O_2 biosensors based on modified Au or glassy carbon electrodes (Table 2). Enzyme-based biosensors are limited by the number of active sites on each, and possibly by stereohindrance when the enzymes are immobilized [46–49]. Also, to avoid loss of activity, enzyme-based sensors must be stored at lower temperatures to avoid enzyme inactivation. Enzyme-free H_2O_2 sensors using metal and metallic oxide particles can overcome such problems and show high stability. They also have rapid response times and lower detection ranges. However, because such materials tend to be poorly adhesive, they must be hybridized with a polymer or electrodeposited directly onto the electrode surface. The polymer PBBI adheres readily to the Au surface and is easily deposited by dropping, dipping or spin coating. Furthermore, there are two reactive imine sites for each repeating unit along the PBBI polymer chain. Finally, altering the morphology of the probe to enhance the surface area can produce a PBBI-modified probe with a short detection time, high sensitivity and good thermal stability.

4. Conclusions

This work uses an electrode material with imine residues that can be oxidized to form *N*-oxide in the presence of AcOH and H_2O_2. This novel mechanism forms the basis for an enzyme-free PBBI/Au electrode to detect H_2O_2. Adding H_2O_2 in PBS that contains AcOH produces AcOOH. PBBI is then oxidized by AcOOH to form PBBINO and AcOH. The PBBINO subsequently reverts to PBBI and water by electrochemical reduction, producing a detectable signal. The intrinsic properties of the polymer make the sensor based on the above mechanism highly selective and stable. Furthermore, the nanoscale environment provided on the surface of the 3D-PBBI/Au electrode greatly enhances the sensitivity (419.4 $\mu A\,mM^{-1}\,cm^{-2}$) and lowers the detection limit to 6.25 μM.

Acknowledgements

We thank the National Science Council of the Republic of China, Chang Gung University, and Chang Gung Memorial Hospital for financial aid: NSC 98-3114-E-182-001-CC2, NSC 94-2216-E-182-001, and CGURPD280091.

References

[1] H. Ohshima, M. Tatemichi, T. Sawa, Arch. Biochem. Biophys. 417 (2003) 3–11.
[2] J. Li, T. Peng, Y. Peng, Electroanalysis 15 (2003) 1031–1037.
[3] T. Endo, R. Ikeda, Y. Yanagida, T. Hatsuzawa, Anal. Chim. Acta 611 (2008) 205–211.
[4] H. Han, Z. Sheng, J. Liang, Anal. Chim. Acta 596 (2007) 73–78.
[5] M. Zayats, R. Baron, I. Popov, I. Willner, Nano Lett. 5 (2005) 21–25.
[6] S. Guo, E. Wang, Anal. Chim. Acta 598 (2007) 181–192.
[7] J.Z. Xu, J.J. Zhu, Q. Wu, Z. Hu, H.Y. Chen, Electroanalysis 15 (2003) 219–224.
[8] X. Chen, C. Fu, Y. Wang, W. Yang, D.G. Evans, Biosens. Bioelectron. 24 (2008) 356–361.
[9] C.Y. Liu, J.M. Hu, Biosens. Bioelectron. 24 (2009) 2149–2154.
[10] J.J. Zhang, Y.G. Liu, L.P. Jiang, J.J. Zhu, Electrochem. Commun. 10 (2008) 355–358.
[11] S. Chakraborty, C.R. Raj, Biosens. Bioelectron. 24 (2009) 3264–3268.
[12] Z. Li, X. Cui, J. Zheng, Q. Wang, Y. Lin, Anal. Chim. Acta 597 (2007) 238–244.
[13] P.C. Pandey, B. Singh, Biosens. Bioelectron. 24 (2008) 842–848.
[14] H. Wang, X. Wang, X. Zhang, X. Qin, Z. Zhao, Z. Miao, N. Huang, Q. Chen, Biosens. Bioelectron. 25 (2009) 142–146.
[15] W. Zhao, H. Wang, X. Qin, X. Wang, Z. Zhao, Z. Miao, L. Chen, M. Shan, Y. Fang, Q. Chen, Talanta 80 (2009) 1029–1033.
[16] S. Wang, L. Lu, M. Yang, Y. Lei, G. Shen, R. Yu, Anal. Chim. Acta 651 (2009) 220–226.
[17] X. Bo, J. Bai, L. Wang, L. Guo, Talanta 81 (2010) 339–345.
[18] M.J. Song, S.W. Hwang, D. Whang, Talanta 80 (2010) 1648–1652.
[19] L. Zhang, H. Li, Y. Ni, J. Li, K. Liao, G. Zhao, Electrochem. Commun. 11 (2009) 812–815.
[20] L.C. Jiang, W.D. Zhang, Electroanalysis 21 (2009) 988–993.
[21] B. Xu, M.L. Ye, Y.X. Yu, W.D. Zhang, Anal. Chim. Acta 674 (2010) 20–26.
[22] Q. Chi, S. Dong, Anal. Chim. Acta 310 (1995) 429–436.
[23] M. Hamer, R.R. Carballo, I.N. Rezzano, Electroanalysis 21 (2009) 2133–2138.
[24] X. Zeng, X. Liu, B. Kong, Y. Wang, W. Wei, Sens. Actuators, B 133 (2008) 381–386.
[25] Y.J. Teng, S.H. Zuo, M.B. Lan, Biosens. Bioelectron. 24 (2009) 1353–1357.
[26] X. Bian, X. Lu, E. Jin, L. Kong, W. Zhang, C. Wang, Talanta 81 (2010) 813–818.
[27] P. Santhosh, K.M. Manesh, A. Gopalan, K.P. Lee, Anal. Chim. Acta 575 (2006) 32–38.
[28] S.A. Kumar, S.M. Chen, J. Mol. Catal. A: Chem. 278 (2007) 244–250.
[29] S.R. Samms, S. Wasmus, R.F. Savinell, J. Electrochem. Soc. 143 (1996) 1225–1232.
[30] I. Yamaguchi, K. Osakada, T. Yamamoto, Macromolecules 30 (1997) 4288–4294.
[31] Q. Li, C. Pan, J.O. Jensen, P. Noyé, N.J. Bjerrum, Chem. Mater. 19 (2007) 350–352.
[32] P. Mustarelli, E. Quartarone, S. Grandi, A. Carollo, A. Magistris, Adv. Mater. 20 (2008) 1339–1343.
[33] A. Sannigrahi, D. Arunbabu, R.M. Sankar, T. Jana, J. Phys. Chem. B 111 (2007) 12124–12132.
[34] H. Pu, G. Liu, Polym. Int. 54 (2005) 175–179.
[35] Y. Iwakura, K. Uno, Y. Imai, J. Polym. Sci. A: Polym. Chem. 2 (1964) 2605–2615.
[36] X. Glipa, B. Bonnet, B. Mula, D.J. Jones, J. Rozière, J. Mater. Chem. 9 (1999) 3045–3049.
[37] K. Nakanishi, P.H. Solomon, Infrared Absorption Spectroscopy, Holden Day, San Francisco, 1977.
[38] C.L. Donnici, D.H.M. Filho, L.L.C. Moreira, G.T. dos Reis, E.S. Cordeiro, I.M.F. de Oliveira, S. Carvalho, E.P. Paniago, J. Brazil Chem. Soc. 9 (1998) 455–460.
[39] T. Sugama, Mater. Lett. 58 (2004) 1307–1312.
[40] I. Losito, C. Malitesta, I. De Bari, C.D. Calvano, Thin Solid Films 473 (2005) 104–113.
[41] M.F. Ryan, R.A. Metcalfe, A.B.P. Lever, M.A. Haga, J. Chem. Soc. Dalton Trans. 14 (2000) 2357–2365.
[42] E. Laviron, J. Electroanal. Chem. 100 (1979) 263–270.
[43] H. Yin, S. Ai, W. Shi, L. Zhu, Sens. Actuators, B: Chem. 137 (2009) 747–753.
[44] E. Laviron, J. Electroanal. Chem. 101 (1979) 19–28.
[45] S. Thiagarajan, S.M. Chen, Talanta 74 (2007) 212–222.
[46] Z. Cao, X. Jiang, Q. Xie, S. Yao, Biosens. Bioelectron. 24 (2008) 222–227.
[47] X. Xu, S. Jiang, Z. Hu, S. Liu, ACS Nano 4 (2010) 4292–4298.
[48] H.Y. Zhao, W. Zheng, Z.X. Meng, H.M. Zhou, X.X. Xu, Z. Li, Y.F. Zheng, Biosens. Bioelectron. 24 (2009) 2352–2357.
[49] L. Zhang, Z. Fang, Y. Ni, G. Zhao, Int. J. Electrochem. Sci. 4 (2009) 407–413.